Nanoscale Advances

ROYAL SOCIETY OF CHEMISTRY

PAPER

View Article Online
View Journal | View Issue

Cite this: *Nanoscale Adv.*, 2020, **2**, 3865

Fabrication of a vanadium nitride/N-doped carbon hollow nanosphere composite as an efficient electrode material for asymmetric supercapacitors†

Xin Jiang,‡[a] Wei Lu,‡[a] Xiaodan Yu,[a] Shuyan Song [b] and Yan Xing *[a]

Low-cost materials and facile processes to obtain novel electrode materials for assembling asymmetric supercapacitors (ASCs) are urgently needed. Herein, a vanadium nitride/nitrogen-doped carbon nanosphere (VN/NCS) composite composed of VN nanoparticles and N-doped carbon (NC) covering the surface of VN has been prepared by the nitridation of a V_2O_3/C nanocomposite. The hollow VN/NCS composite with a mesoporous structure and the dispersion of VN NPs in N-doped carbon result in a VN/NCS composite with good electrochemical behavior. Moreover, the N-doped carbon layer on the surface of VN effectively inhibits the oxidation of VN during cycling in an alkaline electrolyte. With the VN/NC composite utilized as a novel active electrode material for SCs, good rate capability, specific capacitance, and cycling stability are exhibited. Strikingly, using the VN/NCS composite as a negative electrode and its precursor, the V_2O_3/C composite, as a positive electrode, an asymmetric supercapacitor (ASC) device, with a good energy density of 19.8 W h kg^{-1} at 801 W kg^{-1} and a short charging time of 89 s, was assembled.

Received 12th April 2020
Accepted 14th July 2020

DOI: 10.1039/d0na00288g

rsc.li/nanoscale-advances

1. Introduction

The excessive consumption of nonrenewable energy and the ever-growing demand for portable electronics have triggered a great deal of scientific exploration into novel energy storage devices with high power and energy densities.[1–3] Supercapacitors (SCs) have been propelled to the forefront of the field of energy storage due to their considerable merits, such as their high power densities, long cycle lives, fast recharging capabilities, and environmental benignness.[4–6] Nevertheless, the low energy density of SCs severely hinders the commercialization process.[7,8] Therefore, an effective strategy to enhance the energy density while ensuring the power density of SCs is urgently needed. According to the function, $E = 0.5CV^2$, the energy density (E) of SCs can be enhanced by designing a novel nanoscale electrode material with a favorable specific capacitance (C) or broadening the voltage window (V) of SCs.[9,10] The assembly of asymmetric supercapacitors (ASCs) is considered a promising pathway to take full advantage of the voltage windows of both the positive and negative electrodes. As ASC devices are operated at a wide voltage window (up to 2.0 V), an improved energy density could be achieved.[11]

Strikingly, as a novel negative material for SCs, vanadium nitride (VN) has dominated current research because of its high specific capacitance (1340 F g^{-1}), which is higher than that of carbon-based materials. In addition, VN shows better electrical conductivity (1.67×10^6 S m^{-1}) than transition metal oxides,[12–16] hydroxides, and sulfides.[3,6,17–19] Nevertheless, the poor stability of VN in alkaline electrolytes always leads to rapid capacitance fading.[7,8,20] Recently, Ahn *et al.* reported a novel VN/CF structure, with VN nanoparticles (NPs) encapsulated in carbon fiber networks. The structure showed an outstanding specific capacitance of 800 F g^{-1} at a current density of 4 A g^{-1}. Moreover, the assembled VN/CF//$Ni(OH)_2$ ASC device exhibited a favorable energy density and cycling stability.[21] In addition, an intercalation structure with VN NPs incorporated into the GO layer was prepared by Ran *et al.* The obtained VN/GO displayed a good specific capacitance of 109.7 F g^{-1} and excellent cycling stability of 93% capacitance retention after 5000 cycles.[22] Gao *et al.* reported a remarkable strategy for the synthesis of a hybrid electrode composed of VN nanodots intercalated in carbon nanosheets, which displayed a high volumetric capacitance and a favorable cycling stability.[23] Therefore, combining carbon-based material with VN NPs is beneficial for improving the cycling stability and specific capacitance of an electrode material.[24–29]

Based on the above considerations, in this study, a facile template-free solvothermal strategy is utilized for the preparation of spherically structured V_2O_3/C. Vanadium nitride/

[a]Jilin Provincial Key Laboratory of Advanced Energy Materials, Department of Chemistry, Northeast Normal University, Changchun 130024, PR China. E-mail: xingy202@nenu.edu.cn

[b]State Key Laboratory of Rare Earth Resource Utilization, Changchun Institute of Applied Chemistry, Chinese Academy of Sciences, Changchun 130012, P. R. China

† Electronic supplementary information (ESI) available. See DOI: 10.1039/d0na00288g

‡ These authors contributed equally to this work.

nitrogen-doped carbon nanosphere (VN/NCS) composites are obtained *via* the further nitridation of the as-obtained V_2O_3/C precursor. The as-prepared hollow VN/NC nanosphere is composed of numerous VN NPs with a thin nitrogen-doped carbon layer covering the surface of VN. The existence of a nitrogen-doped carbon layer effectively suppresses the oxidation of VN during cycling in alkaline electrolytes, resulting in the improvement of the cycling stability of the electrode material. The hollow cavity and the mesopore of the VN/NCS composite can provide more space for effective electrolyte penetration and rapid ion/electron transportation. Furthermore, the nitrogen-doped carbon helps to enhance the electrical conductivity of the composite. In addition, low-lost vanadium-based oxides have been considered as a class of outstanding pseudocapacitive materials and are widely used in energy storage in view of the rich valence states of vanadium.[30–32] Thus, the V_2O_3/C precursor is used as a positive electrode (0–0.5 V) for assembling an ASC device with VN/NCS as the negative electrode (−1.1 to 0 V). The favorable electrochemical performance of the (+) V_2O_3/C//VN/NCS (−) ASC device is presented.

2. Experimental

2.1 Materials

Ammonium metavanadate (NH_4VO_3) was acquired from Yongda Chemical Reagent Development Center. Glucose ($C_6H_{12}O_6$) and absolute ethanol (CH_3CH_2OH) were purchased from Beijing Chemical Factory.

2.2 Synthesis of the VN/NCS composite

0.25 mol of ammonium metavanadate was dissolved in 20 mL water and ethanol (volume ratio of 3 : 1) solvent mixture. 0.50 mol of glucose was added to 15 mL of water and ethanol (volume ratio of 1 : 2) solvent mixture. Then, the above two solutions were mixed together and transferred into a 50 mL reaction kettle. The solvothermal reaction was kept at 180 °C for 12 h. After centrifugation and washing several times, the black precipitate was dried at 80 °C for 12 h and then heated under an N_2 atmosphere at 700 °C for 1 h, leading to the formation of the V_2O_3/C composite. Finally, the VN/N-doped carbon nanosphere (VN/NCS) composite was obtained by annealing the as-prepared V_2O_3/C nanospheres in an NH_3 atmosphere at 600 °C for 1 h. For comparison, VN nanowires (VN NWs) and N-doped carbon nanospheres (NCS) were also synthesized in the same way without the addition of glucose and ammonium metavanadate, respectively.

The material characterizations and electrochemical measurements are given in ESI.†

3. Results and discussion

A novel VN/NCS nanocomposite was prepared *via* a facile template-free solvothermal method and followed by an annealing process in N_2 and NH_3 atmosphere. The details are presented in Scheme 1. First, the V_2O_3/C hollow nanosphere composite was obtained *via* a solvothermal reaction at 180 °C, followed by a carbon thermal reduction process at 700 °C in a N_2 atmosphere, with NH_4VO_3 as the vanadium source and glucose as both the carbon source and the guiding agent for the spherical structure. Then, the VN/NC nanosphere (VN/NCS) composite was obtained *via* a further nitridation treatment in an NH_3 atmosphere. X-ray powder diffraction (XRD) patterns of bare VN NW, NCS, V_2O_3/C, and VN/NCS composites are given in Fig. 1 and S1.† All of the diffraction peaks in the XRD pattern of the as-prepared V_2O_3/C composite correspond to the V_2O_3 phase (JCPDS 34-0187). The diffraction peaks of the as-prepared VN NWs at around 37.6°, 43.7°, 63.6°, and 76.3° are in good agreement with the (111), (200), (220), and (311) planes of the VN phase (JCPDS 73-2038), respectively. The broad diffraction peak of the N-doped carbon sphere at around 22° is associated with amorphous carbon.[33] The VN/NCS composite shows the diffraction peaks of both VN and the amorphous carbon phase, indicating the coexistence of VN and N-doped carbon.

Furthermore, the surface electronic states of the as-obtained VN/NCS composite were investigated *via* X-ray photoelectron spectroscopy (XPS) (Fig. 2). The XPS C 1s spectrum can be curve-fitted into two peaks with binding energies of 284.6 eV and 285.8 eV, which are attributed to C–C and C–N bonds, respectively. The above result indicates the successful preparation of NC.[5] The N 1s spectrum shows the three chemical states of N, namely quaternary N (400.7 eV), graphitic N (401.1 eV), and

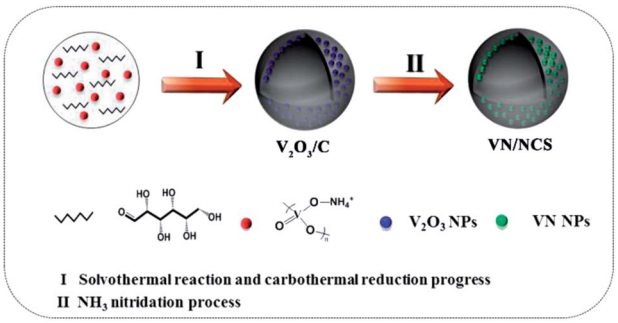

Scheme 1 Schematic representation of the fabrication strategy for the VN/NCS composite.

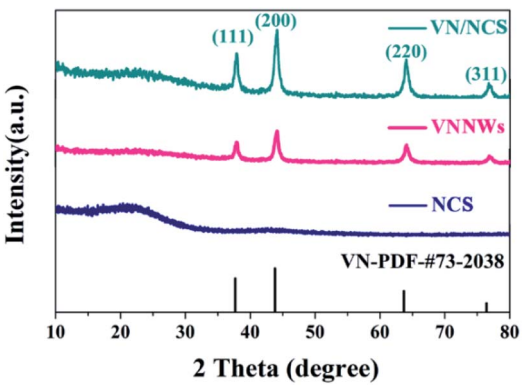

Fig. 1 XRD patterns of the VN, NCS, and VN/NCS nanocomposites.

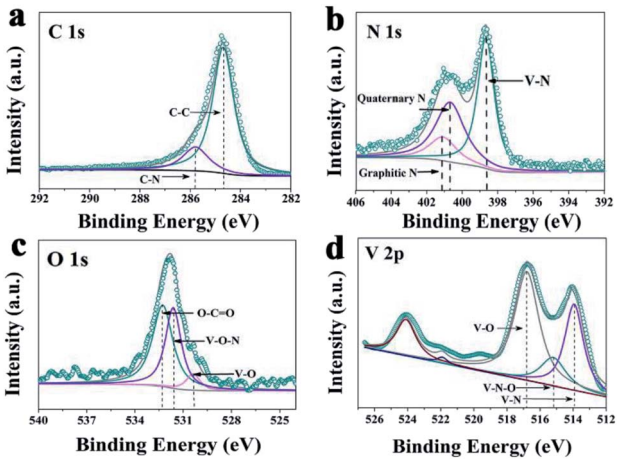

Fig. 2 XPS spectra of (a) C 1s, (b) N 1s, (c) O 1s, and (d) V 2p for the VN/NCS nanocomposite.

metal N (398.7 eV).[34] V 2p in the XPS spectrum is divided into three main peaks: the peak centered at 513.9 eV corresponds to V–N, indicating the formation of VN, while the other two peaks at 515.2 eV and 516.8 eV are assigned to V–N–O and V–O, respectively.[35] In addition, the presence of V–O (530.2 eV) and V–O–N (531.8 eV) bonds in the O 1s spectrum imply the existence of VO_x on the surface of VN.[5,36]

As observed in Fig. S3† and 3a–c, the VN/NCS nanocomposite inherits a sphere-like structure from the V_2O_3/C precursor after the NH_3 reduction treatment. The corresponding magnified scanning electron microscopy (SEM) image (inset in Fig. 3c) demonstrates that the VN/NCS composite has a rough surface and a mean size of 250 nm. Without the addition of NH_4VO_3, the obtained N-doped carbon nanospheres display a smooth surface (Fig. S2a†). Without the presence of glucose, only VN nanowires can be observed in Fig. S2b,† indicating that glucose acts as a guiding agent for the spherical structure. The transmission electron microscopy (TEM) image of the VN/NCS composite in Fig. 3b shows that the as-prepared hollow VN/NC nanosphere is composed of ~20 nm-sized VN NPs, with a thin N-doped carbon layer covering the surface of VN NPs. In the HRTEM image (Fig. 3d), the lattice fringe with a distance of 0.238 nm can be ascribed to the typical (111) crystal plane of cubic VN. In addition, the selected area electron diffraction (SAED) pattern of the VN/NCS nanocomposite (Fig. 3e) shows the good crystallinity of VN NPs. The TEM elemental mapping images of the VN/NCS nanocomposite indicate that the elements of carbon, nitrogen, and vanadium are homogeneously distributed throughout the nanocomposite (Fig. 3f).

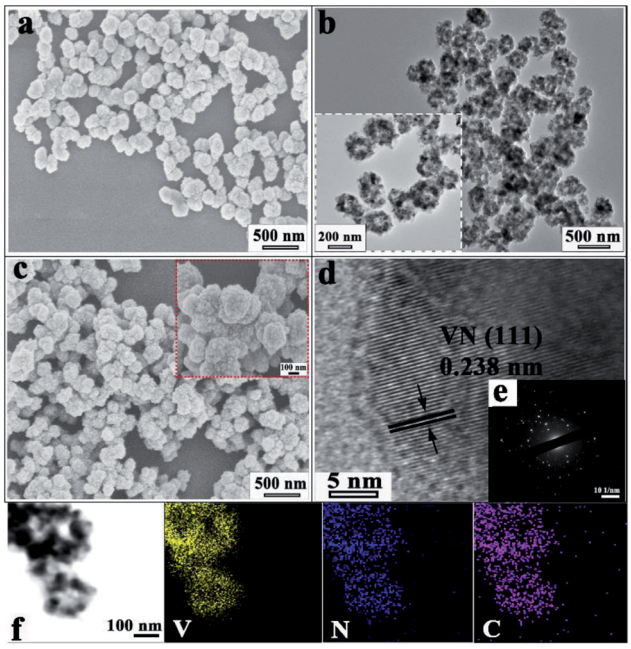

Fig. 3 SEM images of the (a) V_2O_3/C and (c) VN/NCS nanocomposites, (b) TEM image, (d) HRTEM image, (e) SAED pattern, and (f) TEM mapping images of the VN/NCS nanocomposite.

The N_2 adsorption–desorption isotherms of the VN/NCS nanocomposite in Fig. 4 show a typical IV isotherm with an H_3-type hysteresis loop, indicating the mesoporous feature of the composite. The abundant mesopores with wide pore size distributions (inset in Fig. 4) will endow the VN/NCS electrode with more effective electrolyte penetration and rapid ion/electron transportation, leading to good electrochemical behavior.[37,38]

The capacitive properties of the VN NW, NCS, and VN/NCS electrodes were tested on a three-electrode system in a 2 M KOH electrolyte. As observed in Fig. 5a, the cyclic voltammetry (CV) curve of the VN/NCS electrode shows redox peaks, which indicate that the capacitive mechanism in VN/NCS consists of faradaic reactions,[21] and the dispersion of VN NPs in N-doped carbon results in more exposed VN active sites, leading to a larger CV curve area than that of VN NWs and NCS. The C_s values of the VN NW, NCS, and VN/NCS composites calculated from the galvanostatic charge–discharge (GCD) curves (Fig. 5b) are 54 F g^{-1}, 76 F g^{-1}, and 148 F g^{-1}, respectively, suggesting the favorable capacitance performance of the VN/NCS composite. As listed in Table 1, the C_s of the VN/NCS electrode is better than that of reported metal nitride-based electrodes or carbon-based

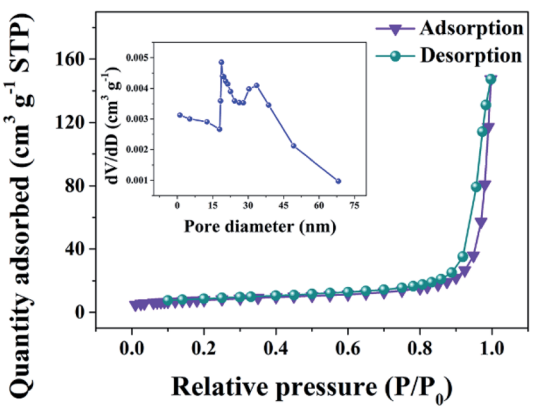

Fig. 4 Nitrogen adsorption–desorption isotherms and the corresponding pore size distribution curve (inset) of the VN/NCS nanocomposite.

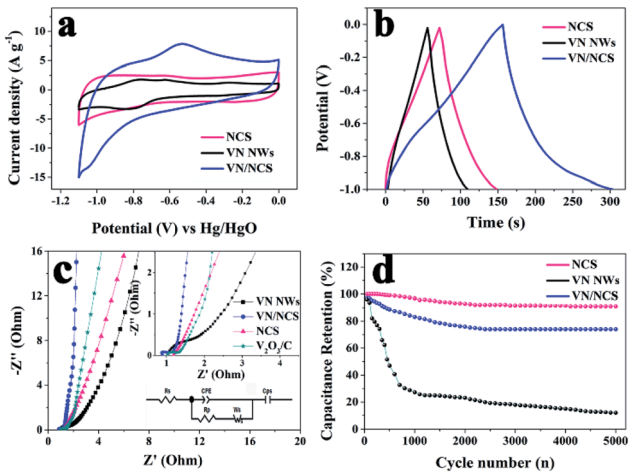

Fig. 5 (a) CV curves and (b) GCD curves of the VN NW, NCS, and VN/NCS electrodes, (c) Nyquist plots of the VN NW, NCS, VN/NCS, and V_2O_3/C electrodes with the equivalent circuit of the VN/NCS electrode from impedance spectroscopic analysis and (d) long-term cycling stability at a current density of 10 A g^{-1} for the VN NW, NCS, and VN/NCS electrodes.

Table 1 Comparison of the specific capacitance of the VN/NCS electrode with that of previously reported electrodes

Samples	Current density (A g^{-1})	Specific capacitance (F g^{-1})	Ref.
Urchin-like VN	0.5	98.5	9
Ni/VN	0.5	143.2	11
VN/GO	1.0	109.7	22
VN/V_2O_3/C	0.5	138.0	24
Mo_2N@PANI	0.5	111.8	40
VN/NCS	1.0	148.0	This work

electrodes.[9,11,22,24,40] Moreover, the Nyquist plots of the VN/NCS, VN NW, and NCS electrodes obtained *via* electrochemical impedance spectroscopy (EIS), and the equivalent circuit of the VN/NCS electrode are shown in Fig. 5c. C_{ps} and CPE refer to the pseudocapacitive element from the redox process of VN and the constant phase element involving the double-layer capacitance, respectively. The Nyquist plot of the VN/NCS electrode has a steeper slope, lower intercept with the *x*-axis, and smaller semicircle loop that the VN NW and NCS electrodes. This results in better capacitive behavior, lower intrinsic resistance (R_s), and lower charge transfer resistance (R_{ct}),[41,42] resulting in the better electrical conductivity of the VN/NCS electrode compared to that of the VN NW and NCS electrodes.[28,34] In addition to the favorable capacitance performance and electrical conductivity, the VN/NCS electrode also exhibits good cycling stability of 78% capacitance retention at a current density of 10 A g^{-1} after 5000 cycles. Comparatively, VN NWs show very poor stability after a 5000 cycle test, suggesting that the NC layer on the surface of VN is good for the cycling stability of the active electrode (Fig. 5d). Moreover, the capacitive contribution is associated with a fast-electrochemical process including the ion adsorption/desorption process of NC and fast faradaic reactions of VN NPs.[43] As observed in Fig. 6, the VN/NCS electrode has a capacitive contribution of 52%, which is much higher than that of the NCS electrode (14%) and the VN NW electrode (18%), indicating the good capacitance behavior of the VN/NCS electrode, which may be ascribed to the synergistic effect between N-doped carbon and VN NPs. The above results are consistent with the CV and GCD results. Furthermore, CV and GCD tests at various scan rates and current densities were further performed to access the rate capability of the VN/NCS electrode. As shown in Fig. 7a, the CV curve of the VN/NCS electrode remains its original shape even at a high scan rate of 500 mV s^{-1}, implying the excellent rate capability of the VN/NCS electrode. The GCD curves of the VN/NCS electrode (Fig. 7c) measured at various current densities (0.5–20 A g^{-1}) exhibit a nearly symmetrical triangle, implying the good charge–discharge reversibility of the composite electrode. In addition, the coulombic efficiency of the VN/NCS electrode (in Fig. S4†) at a current density of 20 A g^{-1} is 98.5%, confirming good electrochemical reversibility. The favorable electrochemical properties of the VN/NCS composite may be ascribed to the following reasons: (I) the dispersion of VN NPs in N-doped carbon results in more exposed VN active sites, leading to a good specific capacitance; (II) quaternary N and graphitic N in the N-doped carbon are beneficial for the improvement of the electrical conductivity for the electrode material;[5,39] (III) the mesoporous structure and hollow cavities of VN/NCS endow the composite electrode with more effective electrolyte penetration and rapid ion/electron transportation, leading to good electrochemical behavior; (IV) the thin layer of NC on the surface of VN NPs effectively inhibits the oxidation of VN NPs, thus producing excellent cycling stability.

Strikingly, in our study, the V_2O_3/C composite is utilized not only as a precursor for the fabrication of the VN/NCS composite but also as a positive electrode for the assembling the ASC device. The CV curves of the V_2O_3/C electrode at different scan rates shown in Fig. 7b suggest a good rate capability for V_2O_3/C.

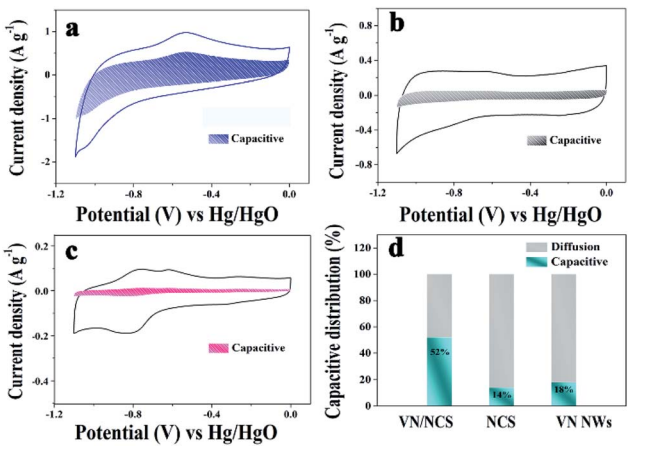

Fig. 6 Capacitive contribution of the (a) VN/NCS; (b) NCS, and (c) VN NW electrodes at a scan rate of 5 mV s^{-1}; (d) capacitive and diffusion-controlled contribution fractions of the VN/NCS, NCS, and VN NW electrodes at a scan rate of 5 mV s^{-1}.

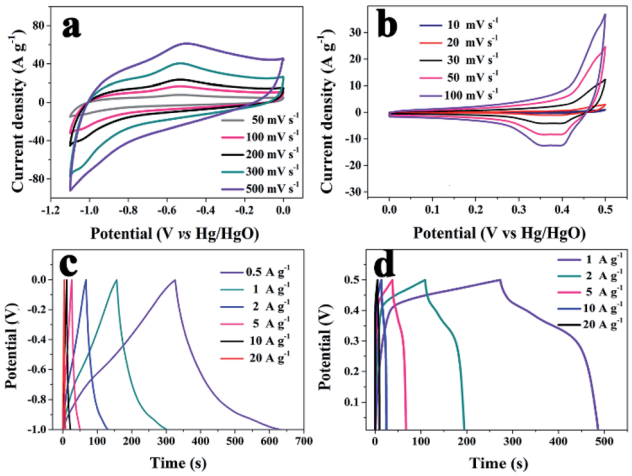

Fig. 7 CV curves, at various scan rates, of the (a) VN/NCS electrode and (b) V_2O_3/C electrode; GCD curves at various current densities for the (c) VN/NCS electrode and (d) V_2O_3/C electrode.

As calculated from Fig. 7d, C_s of the V_2O_3/C electrode is 431 F g^{-1} at 1 A g^{-1} and a C_s of 199 F g^{-1} is maintained even at a high current density of 20 A g^{-1}. In addition, the EIS test of the V_2O_3/C composite in Fig. 5c indicates favorable electrical conductivity.

Based on the good electrochemical behavior of the V_2O_3/C positive and VN/NCS negative electrodes, an ASC device was established. As shown in Fig. 8a, the voltage window of the (+) V_2O_3/C//VN/NCS (−) ASC device could reach 1.6 V, which is beyond that of most traditional symmetrical supercapacitors (~1.0 V). GCD tests in various voltage windows were carried out at 1 A g^{-1} (Fig. 8c) and C_s increased from 40 to 59 F g^{-1} with the increase in the voltage window from 1.0 V to 1.6 V owing to the occurrence of continuous redox reactions between two active electrodes in the KOH electrolyte. In addition, the CV curves measured at various scan rates in a two-electrode system are exhibited in Fig. 8b. The shape of the CV curves for the two-electrode system is slightly different from that of the V_2O_3/C and VN/NCS electrodes, which may be ascribed to the synergistic effect between the V_2O_3/C and VN/NCS electrodes.[10] C_s of the ASC device calculated from the GCD curve in Fig. 8d is 59 F g^{-1} at 1 A g^{-1} and was maintained at 18 F g^{-1} at a high current density of 10 A g^{-1}, testifying the favorable rate capability of the assembled two-electrode system. In addition, the coulombic efficiency of the ASC device at the current density ranger of 1–10 A g^{-1} is observed in Fig. S5a.†

At a low current density of 1 A g^{-1}, the assembled ASC device exhibits a low coulombic efficiency, which may be ascribed to adverse reactions involving the two electrodes and the electrolyte, resulting in an incomplete discharge process.[28] As the current density increases, the charge–discharge time decreases and the electrochemical process is mainly affected by the electric double layer, thus the coulombic efficiency becomes higher.[28] Moreover, a good energy density of 19.8 W h kg^{-1} and a power density of 801 W kg^{-1} are observed in the Ragone plots (power density *vs.* energy density *vs.* charge time) for the (+) V_2O_3/C//VN/NCS (−) ASC device, as illustrated in Fig. 9, and the corresponding charging time is only 89 s. Even with a shortened charging time of 4 s, a good energy density of 6.6 W h kg^{-1} at 7680 W kg^{-1} can be achieved. In addition, the cycling test results for the (+) V_2O_3/C//VN/NCS (−) ASC device reflect relatively good long cycle stability with an initial capacitance retention of 66.5% after 5000 cycles (Fig. S5b†). In addition, the Nyquist plots from the impedance spectroscopic analysis with the equivalent circuit for the ASC device before and after cycling have also been tested. As shown in Fig. S6,† there is no obvious increase in the internal resistance (R_s), indicating good contact between the electrode material and current collector over the cycle test.[44] Therefore, vanadium-based oxide and nitride are considered to be a class of novel electrode materials with excellent power and energy densities for SCs.

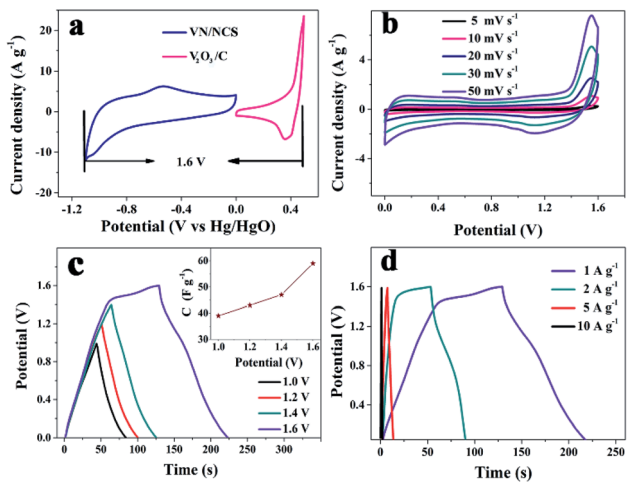

Fig. 8 (a) CV curves of the V_2O_3/C and VN/NCS electrodes at a scan rate of 50 mV s^{-1} in a three electrode system with 2 M KOH as the electrolyte. The electrochemical performances of the assembled ASC device: (b) CV curves of the two-electrode system at different scan rates in a voltage window of 1.6 V, (c) GCD curves in different voltage windows at a current density of 1 A g^{-1}, (d) GCD curves at various current densities.

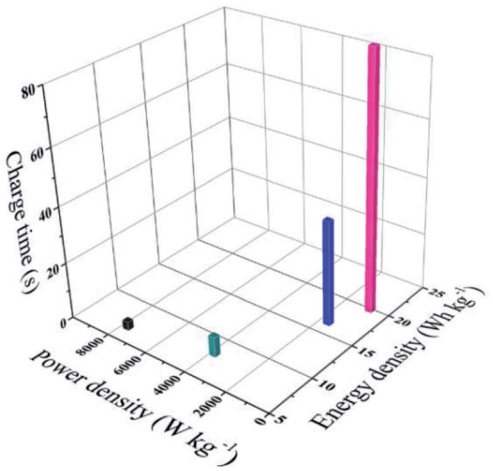

Fig. 9 Ragone plot of the ASC device (energy density *vs.* power density *vs.* charge time).

4. Conclusions

In summary, a VN/NCS composite composed of VN NPs and N-doped carbon covering on the surface of VN was successfully prepared by the nitridation of the V_2O_3/C precursor. As the VN/NCS composite was used as a negative electrode for SCs, favorable rate capability and specific capacitance were attained in view of the synergistic effect between VN NPs and N-doped carbon. More significantly, an ASC device was established with V_2O_3/C as the positive electrode and VN/NCS as the negative electrode and excellent energy density of 19.8 W h kg^{-1} at a power density of 801 W kg^{-1} was achieved. This study has set up a novel concept for the fabrication of both positive and negative electrodes with low-cost materials as promising candidates for ASC devices in the energy storage field.

Conflicts of interest

There are no conflicts to declare.

Acknowledgements

This work was supported by the National Natural Science Foundation of China (Grant No. 21872023) and Opening Fund of State Key Laboratory of Rare Earth Resource Utilization.

Notes and references

1 A. González, E. Goikolea, J. A. Barrena and R. Mysyk, Review on supercapacitors: Technologies and materials, *Renewable Sustainable Energy Rev.*, 2016, **58**, 1189–1206.
2 K. Robert, D. Deresmes, C. Douard, A. Ladecola, P. Roussel, T. Brousse and C. Lethien, Novel insights into the charge storage mechanism in pseudocapacitive vanadium nitride thick films for high-performance on-chip micro-supercapacitors, *Energy Environ. Sci.*, 2020, **13**, 949–957.
3 J. F. Sun, C. Wu, X. F. Sun, H. Hu, C. Y. Zhi, L. R. Hou and C. Z. Yuan, Recent progresses in high-energy-density all pseudocapacitive-electrode-materials-based asymmetric supercapacitors, *J. Mater. Chem. A*, 2017, **5**, 9443.
4 L. F. Chen, Y. Lu, L. Yu and X. W. Lou, Designed formation of hollow particle-based nitrogen-doped carbon nanofibers for high-performance supercapacitors, *Energy Environ. Sci.*, 2017, **10**, 1777.
5 H. H. Liu, H. L. Zhang, H. B. Xu, T. P. Lou, Z. T. Sui and Y. Zhang, *In situ* self-sacrificed template synthesis of vanadium nitride/nitrogen-doped graphene nanocomposites for electrochemical capacitors, *Nanoscale*, 2018, **10**, 5246–5253.
6 P. B. Geng, S. S. Zheng, H. Tang, R. M. Zhu, L. Zhang, S. Cao, H. G. Xue and H. Pang, Transition metal sulfides based on graphene for electrochemical energy storage, *Adv. Energy Mater.*, 2018, **8**, 1703259.
7 M. Balogun, W. Qiu, W. Wang, P. Fang, X. Lu and Y. Tong, Recent advances in metal nitrides as high-performance electrode materials for energy storage devices, *J. Mater. Chem. A*, 2015, **3**, 1364.
8 B. Gao, X. X. Li, K. Ding, C. Huang, Q. W. Li, P. K. Chu and K. F. Huo, Recent progress in nanostructured transition metal nitrides for advanced electrochemical energy storage, *J. Mater. Chem. A*, 2019, **7**, 14.
9 R. Wang, X. Yan, J. Lang, Z. Zheng and P. Zhang, A hybrid supercapacitor based on flower-like $Co(OH)_2$ and urchin-like VN electrode materials, *J. Mater. Chem. A*, 2014, **2**, 12724.
10 J. Zhao, C. Li, Q. Zhang, J. Zhang, X. Wang, Z. Lin, J. Wang, W. Lv, C. Lu, C. Wong and Y. Yao, An all-solid-state, lightweight, and flexible asymmetric supercapacitor based on cabbage-like $ZnCo_2O_4$ and porous VN nanowires electrode materials, *J. Mater. Chem. A*, 2017, **5**, 6928.
11 C. Ji, J. Bi, S. Wang, X. Zhang and S. Yang, Ni nanoparticle doped porous VN nanoflakes assembled into hierarchical hollow microspheres with a structural inheritance from the $Ni_{1-x}V_xO_2$ cathode material for high performance asymmetric supercapacitors, *J. Mater. Chem. A*, 2016, **4**, 2158.
12 R. J. Lin, Z. N. Li, D. I. Amaiem, B. J. Zhang, D. J. L. Brett, G. J. He and I. P. Parkin, A general method for boosting the supercapacitor performance of graphitic carbon nitride/graphene hybrids, *J. Mater. Chem. A*, 2017, **5**, 25545.
13 J. Hu, P. Yang, S. H. Wang and J. J. Shi, Synthesis of Micro/Nano-Flower Ni_xCo-P-O for High-Performance Electrochemical Supercapacitors, *ChemElectroChem*, 2019, **6**, 928–936.
14 X. X. Li, J. J. Fu, Z. G. Pan, J. J. Su, J. W. Xu, B. Gao, X. Peng, L. Wang, X. M. Zhang and P. K. Chu, Peapod-like V_2O_3 nanorods encapsulated into carbon as binder-free and flexible electrodes in lithium-ion batteries, *J. Power Sources*, 2016, **311**, 58.
15 R. S. Kate, S. A. Khalate and R. J. Deokate, Overview of nanostructured metal oxides and pure nickel oxide (NiO) electrodes for supercapacitors: A review, *J. Alloys Compd.*, 2018, **734**, 89–111.
16 T. Hu, Y. Y. Liu, Y. F. Zhang, Y. Nie, J. Q. Zheng, Q. S. Wang, H. M. Jiang and C. G. Meng, Encapsulating V_2O_3 nanorods into carbon core-shell composites with porous structures and large specific surface area for high performance solid-state supercapacitors, *Microporous Mesoporous Mater.*, 2018, **262**, 199–206.
17 H. Pang, X. R. Li, Q. X. Zhao, H. G. Xue, W. Y. Lai, Z. Hu and W. Huang, One-pot synthesis of heterogeneous Co_3O_4-nanocube/$Co(OH)_2$-nanosheet hybrids for high-performance flexible asymmetric all-solid-state supercapacitors, *Nano Energy*, 2017, **35**, 138–145.
18 Y. M. Chen, Z. Li and X. W. Lou, General formation of $M_xCo_{3-x}S_4$ (M = Ni, Mn, Zn) hollow tubular structures for hybrid supercapacitors, *Angew. Chem.*, 2015, **127**, 10667–10670.
19 H. Liu, H. Guo, L. G. Yue, N. Wu, Q. Li, W. Q. Yao, R. Xue, M. Y. Wang and W. Yang, Metal-Organic Frameworks-Derived NiS_2/CoS_2/N-Doped Carbon Composites as Electrode Materials for Asymmetric Supercapacitor, *ChemElectroChem*, 2019, **6**, 3764–3773.
20 Y. L. Xu, J. Wang, L. F. Shen, H. Dou and X. G. Zhang, One-Dimensional Vanadium Nitride Nanofibers Fabricated by Electrospinning for Supercapacitors, *Electrochim. Acta*, 2015, **173**, 680–686.

21 G. H. An, D. Y. Lee and H. J. Ahn, Vanadium nitride encapsulated carbon fibre networks with furrowed porous surfaces for ultrafast asymmetric supercapacitors with robust cycle life, *J. Mater. Chem. A*, 2017, **5**, 19714.

22 T. He, Z. Wang, X. Li, Y. Tan, Y. Liu, L. Kong, L. Kang, C. Chen and F. Ran, Intercalation structure of vanadium nitride nanoparticles growing on graphene surface toward high negative active material for supercapacitor utilization, *J. Alloys Compd.*, 2019, **781**, 1054.

23 Q. Li, Y. Chen, J. Zhang, W. Tian, L. Wang, Z. Ren, X. Ren, X. Li, B. Gao, X. Peng, P. K. Chu and K. Huo, Spatially confined synthesis of vanadium nitride nanodots intercalated carbon nanosheets with ultrahigh volumetric capacitance and long life for flexible supercapacitors, *Nano Energy*, 2018, **51**, 128.

24 Y. F. Zhang, X. W. Wang, J. Q. Zheng, T. Hu, X. Liu and C. G. Meng, Facile synthesis of high-surface vanadium nitride/vanadium sesquioxide/amorphous carbon composite with porous structures as electrode materials for high performance symmetric supercapacitors, *Appl. Surf. Sci.*, 2019, **471**, 842–851.

25 Y. Liu, Q. H. Wu, L. Y. Liu, P. Manasa, L. Kang and F. Ran, Vanadium Nitride for Aqueous Supercapacitors: A Topic Review, *J. Mater. Chem. A*, 2020, **8**, 8218–8233.

26 Y. Liu, L. Liu, L. Kong, L. Kang and F. Ran, Supercapacitor Electrode Based on Nano-Vanadium Nitride Incorporated on Porous Carbon Nanospheres Derived from Ionic Amphiphilic Block Copolymers & Vanadium-Contained Ion Assembly Systems, *Electrochim. Acta*, 2016, **211**, 469.

27 Y. Liu, L. Liu, Y. Tan, L. Niu, L. Kong, L. Kang and F. Ran, Carbon nanosphere@vanadium nitride electrode materials derived from metal-organic nanospheres self-assembled by NH_4VO_3, chitosan, and amphiphilic block copolymer, *Electrochim. Acta*, 2018, **262**, 66.

28 Y. Yang, L. Zhao, K. Shen, Y. Liu, X. Zhao, Y. Wu, Y. Wang and F. Ran, Ultra-small vanadium nitride quantum dots embedded in porous carbon as high performance electrode materials for capacitive energy storage, *J. Power Sources*, 2016, **333**, 61.

29 Y. Yang, K. Shen, Y. Liu, Y. Tan, X. Zhao, J. Wu, X. Niu and F. Ran, Novel Hybrid Nanoparticles of Vanadium Nitride/Porous Carbon as an Anode Material for Symmetrical Supercapacitor, *Nano-Micro Lett.*, 2017, **9**, 6.

30 M. S. Javed, H. Lei, Z. L. Wang, B. T. Liu, X. Cai and W. J. Mai, 2D V_2O_5 Nanosheets as a Binder-free High-energy Cathode for Ultrafast Aqueous and Flexible Zn-ion Batteries, *Nano Energy*, 2020, **70**, 104573.

31 H. Y. Li, K. Jiao, L. Wang, C. Wei, X. L. Li and B. Xie, Micelle anchored *in situ* synthesis of V_2O_3 nanoflakes@C composites for supercapacitors, *J. Mater. Chem. A*, 2014, **2**, 18806–18815.

32 Y. F. Zhang, J. Q. Zheng, X. Y. Jing and C. G. Meng, A strategy for the synthesis of VN@C and VC@C core–shell composites with hierarchically porous structures and large specific surface areas for high performance symmetric supercapacitors, *Dalton Trans.*, 2018, **47**, 8052.

33 B. Long, M. S. Balogun, L. Luo, Y. Luo, W. T. Qiu, S. Q. Song, L. Zhang and Y. X. Tong, Encapsulated Vanadium-Based Hybrids in Amorphous N-Doped Carbon Matrix as Anode Materials for Lithium-Ion Batteries, *Small*, 2017, **13**, 1702081.

34 Y. Wu and F. Ran, Vanadium nitride quantum dot/nitrogen-doped microporous carbon nanofibers electrode for high-performance supercapacitors, *J. Power Sources*, 2017, **344**, 1.

35 J. Huang, Z. Y. Peng, Y. B. Xiao, Y. Z. Xu, L. F. Chen, Y. S. Xiong, L. C. Tan, K. Yuan and Y. W. Chen, Hierarchical Nanosheets/Walls Structured Carbon-Coated Porous Vanadium Nitride Anodes Enable Wide-Voltage-Window Aqueous Asymmetric Supercapacitors with High Energy Density, *Adv. Sci.*, 2019, **6**, 1900550.

36 X. N. Wang, J. Sun, J. X. Zhao, Z. Y. Zhou, Q. C. Zhang, C. P. Wong and Y. G. Yao, All-Solid-State Fiber-Shaped Asymmetric Supercapacitors with Ultrahigh Energy Density Based on Porous Vanadium Nitride Nanowires and Ultrathin $Ni(OH)_2$ Nanosheet Wrapped $NiCo_2O_4$ Nanowires Arrays Electrode, *J. Phys. Chem. C*, 2019, **123**, 985–993.

37 J. Yuan, X. Hu, J. X. Chen, Y. J. Liu, T. Z. Huang and Z. H. Wen, *In situ* formation of vanadium nitride quantum dots on N-doped carbon hollow spheres for superior lithium and sodium storage, *J. Mater. Chem. A*, 2019, **7**, 9289.

38 T. N. Tran, C. H. Shin, B. J. Lee, J. Samdani, J. D. Park, T. H. Kang and J. S. Yu, Fe-N-functionalized carbon electrocatalyst derived from zeolitic imidazolate framework for oxygen reduction: Fe and NH_3 treatment effects, *Catal. Sci. Technol.*, 2018, **8**, 5368–5381.

39 L. Chen, X. Zhang, H. Liang, M. Kong, Q. Guan, P. Chen, Z. Wu and S. Yu, Synthesis of Nitrogen-Doped Porous Carbon Nanofibers as an Efficient Electrode Material for Supercapacitors, *ACS Nano*, 2012, **6**, 7092.

40 T. Q. He, W. L. Zhang, P. Manasa and F. Ran, Quantum dots of molybdenum nitride embedded in continuously distributed polyaniline as novel electrode material for supercapacitor, *J. Alloys Compd.*, 2020, **812**, 152138.

41 Y. Cheng, Y. F. Zhang, H. M. Jiang and Z. K. Kou, Coupled cobalt silicate nanobelt-on-nanobelt hierarchy structure with reduced graphene oxide for enhanced supercapacitive performance, *J. Power Sources*, 2020, **448**, 227407.

42 J. Q. Zheng, Y. F. Zhang, C. G. Meng and G. Z. Cao, V_2O_3/C nanocomposites with interface defects for enhanced intercalation pseudocapacitance, *Electrochim. Acta*, 2019, **318**, 635–643.

43 Y. Abbas, S. N. Yun, M. S. Javed and J. G. Chen, Anchoring 2D $NiMoO_4$ nano-plates on flexible carbon cloth as a binder-free electrode for efficient energy storage devices, *Ceram. Int.*, 2019, **46**, 4470–4476.

44 M. S. Javed, S. G. Dai, M. J. Wang, D. L. Guo, L. Chen, X. Wang, C. G. Hu and Y. Xi, High performance solid state flexible supercapacitor based on molybdenum sulfide hierarchical nanospheres, *J. Power Sources*, 2015, **285**, 63–69.